Pseudomonas aeruginosa PA14 produces R-bodies, extendable protein polymers with roles in host colonization and virulence

Bryan Wang[1], Yu-Cheng Lin[1], Jeanyoung Jo[1], Alexa Price-Whelan[1], Shujuan Tao McDonald [1,2], Lewis M. Brown[1,2], and Lars E.P. Dietrich[1]*

[1]Department of Biological Sciences, Columbia University, New York, NY, USA
[2]Quantitative Proteomics and Metabolomics Center, Columbia University, New York, NY, USA

*email: LDietrich@columbia.edu

Abstract

Pseudomonas aeruginosa causes biofilm-based infections in diverse hosts. A majority of sequenced *P. aeruginosa* genomes, including that of the popular model strain UCBPP-PA14 ("PA14"), contain a gene cluster with the potential to confer production of large, extendable protein polymers called R-bodies. R-bodies are best known for their role in killing of paramecia by the bacterium *Caedibacter taeniospiralis*, and genes in PA14's R-body-associated cluster had previously been linked to its virulence. However, the ability to produce R-bodies had not been investigated in this strain. Here we show that R-bodies are among the most abundant proteins present in SDS-insoluble preparations from PA14 biofilms and that two adjacent regulatory genes, including the gene coding for the sigma factor FecI2, are required for expression of R-body structural genes. Subpopulations of PA14 cells express R-body structural genes during biofilm growth and during colonization of plant and animal hosts. Moreover, R-body production is required for wild-type levels of colonization of *A. thaliana* seedlings and full virulence in a *C. elegans* killing assay. Our results suggest that R-body production may contribute to the observed differences in virulence among *P. aeruginosa* isolates.

Introduction

R-bodies are enigmatic biological machines that have been characterized most extensively in *Caedibacter taeniospiralis*, an obligate endosymbiont of paramecia. These structures are composed of ~ 12 kDa monomers that polymerize to form hypercoiled ribbons ~ 0.5 µm in diameter [1]. In response to changes in parameters such as pH, temperature, or ionic strength [2–4], R-body coils extend into 10-20-µm-long needle-like structures (i.e., ~ 10X the length of the producing cell), lysing the bacterium [4,5]. In the *Caedibacter-Paramecium* endosymbiosis, tolerant host paramecia shed *C. taeniospiralis* into the environment, where the bacteria can be taken up by neighboring, sensitive paramecia. R-body-mediated lysis is triggered by lysosomal conditions and thought to release an unidentified factor that is toxic to sensitive paramecia. R-body-producing endosymbionts therefore confer onto their host cell a "killing" phenotype and a competitive advantage in a phenomenon that was first described by Tracy M. Sonneborn in 1938 [6]. Subsequent genetic studies have implicated three genes--*rebA, B,* and *D*--in *C. taeniospiralis* R-body production. Oddly, RebA, B, and D are all homologous to each other, but RebA and RebB constitute the primary *C. taeniospiralis* R-body components [7–9].

The opportunistic pathogen *Pseudomonas aeruginosa* is a major cause of biofilm-based infections. A substantial fraction (147/241) of *P. aeruginosa* complete strain genomes, including that of strain UCBPP-PA14 ("PA14"), contain *reb* gene homologs as part of a cluster that includes the gene for the sigma factor FecI2 and targets of FecI2 [10]; we refer to this region as the "*reb* cluster". Genes in the *reb* cluster have been identified as contributing to increased virulence when distinct *P. aeruginosa* isolates are compared [11,12]. Notably, the popular model strain PAO1 does not contain a *reb* cluster and this is consistent with its relatively low virulence in a *Caenorhabditis elegans* infection assay. These observations, combined with the known contributions of R-bodies to host damage in other systems [4,13,14], led us to hypothesize that PA14 produces R-bodies that contribute to pathogenicity.

In this report we detail characteristics of the PA14 *reb* cluster. We provide evidence of R-body production by PA14 biofilms and show that PA14 *rebP1P2*, an operon encoding *C. taeniospiralis reb* gene homologs, is required for this. We also find that cells in PA14 liquid cultures and biofilms exhibit stochastic P_{rebP1} expression that is dependent on local regulatory genes and that this promoter is active during interactions with *Arabidopsis thaliana* and *Caenorhabditis elegans* hosts. Finally, we show that *rebP1P2* is necessary for wild type-like levels of colonization of *A. thaliana* seedlings and virulence in *C. elegans*. Together, these findings raise the possibility that R-body production is a component of the marked strain-dependent variation in pathogenicity observed for *P. aeruginosa* [15].

Results

Phylogenetic analysis of pseudomonad R-body-associated genes and description of the PA14 reb *cluster*

A previous analysis showed that homologs of *C. taeniospiralis reb* genes are broadly distributed throughout the proteobacterial clade [16]. To investigate the phylogenetic relationships between Reb homologs from proteobacterial genomes, we BLASTed PA14_27640, which is the PA14 protein most similar to *C. taeniospiralis* RebB*,* against all complete bacterial genomes used for the prior analyses conducted by [16] plus 14 representative pseudomonads. We generated a tree that shows the relationships of all Reb homologs from these proteobacteria (**Figure 1a**). In this tree, *C. taeniospiralis* RebA and RebB form a distinct grouping and are closely related to Reb homologs from non-pseudomonad gammaproteobacteria, such as those in the genera

Shewanella and *Allivibrio* (**Supplementary Figure 1**). Reb homologs from pseudomonads fall into two groups: (i) one that contains *C. taeniospiralis* RebD and PA14_27685 and for which we have therefore designated its members as "RebD"; and (ii) one that is distinct from the *C. taeniospiralis* Rebs but that includes representatives from many *reb* cluster-containing pseudomonads and chromobacteria, and for which we have therefore designated its members as "RebP". The two *rebP* homologs present in PA14, *PA14_27640* and *PA14_27630*, are predicted to form an operon that we refer to as *rebP1P2*.

We examined the chromosomal regions of representative pseudomonad strains that contain *rebD* and *rebP1P2* and refer to the strain-specific groups of genes in these loci as "*reb* clusters". In pseudomonads that contain *rebD* and *rebP1P2*, there are three additional ORFs that are well-conserved. These include two regulatory genes, *PA14_27700* and *fecI2*, which code for a transcription factor and sigma factor, respectively, and which in a prior study were required for full virulence in a *C. elegans* killing assay [17] (**Figure 1b**). We have given *PA14_27700* the designation "*rcgA"* (for *reb* cluster gene A). The third gene, *PA14_27680*, was previously shown (together with *PA14_27700*) to contribute to PA14's enhanced virulence when it was compared to *P. aeruginosa* strain PAO1 in *C. elegans* infection studies [11]. *PA14_27680* is conserved in all pseudomonads that contain at least one *reb* structural gene, suggesting that it may be associated with R-body function and we have therefore named it "*rapA"* (R-body-associated protein A). Although *rebP* homologs are scattered across the phylogenetic tree of the genus *Pseudomonas* (**Supplementary Figure 2**), homologs of the regulatory genes show strong conservation in strains that contain *rebP* genes, both within the species *P. aeruginosa* (in 146/147 *rebP*-containing genomes; **Supplementary File 1**) and among other pseudomonads (**Figure 1b**).

PA14 cells growing in biofilms produce R-bodies

For most bacteria that contain *reb* genes, the ability to produce R-bodies has not been investigated. To determine whether PA14 produces R-bodies, we applied a modified R-body enrichment protocol [18] to biofilms formed by the WT and by Δ*pel*, a mutant that is unable to produce the major PA14 exopolysaccharide and that therefore yields biofilms that are more amenable to disruption. We performed protein mass spectrometry (MS) and scanning-electron microscopy (SEM) on the isolated SDS-insoluble fractions (**Figure 2a**). Strikingly, three products of the *reb* cluster—RapA, RebP1, and RebP2–were detected by MS at similar levels

and were among the 12 most abundant proteins in our sample (**Figure 2b**). One other uncharacterized protein coded for by the *reb* gene cluster, PA14_27675, was also detected specifically in the SDS-insoluble fractions prepared from Δ*pel* biofilms and at levels two times lower than RebP1 and RebP2 (PA14_27675 was not detected in preparations from WT biofilms) (**Figure 2b**). Consistent with the MS results, our SEM analyses revealed the presence of R-bodies in preparations from WT PA14 biofilms (**Figure 2c**). We detected R-bodies in various states ranging from hypercoiled (~ 450 nm long) to extended (~ 5.5 µm long) (**Figure 2c, d, e**). These structures were not observed in a deletion mutant lacking the *rebP1P2* operon (Δ*rebP1P2*) (**Supplementary Figure 3**). Taken together, our data indicate that R-bodies are produced by PA14 biofilms.

rebP1P2 *expression is stochastic and dependent on RcgA and FecI2, in both liquid cultures and biofilms*

Having observed that *rebP1P2* is required for R-body production by PA14 biofilms, we sought to characterize the expression of this locus. We generated a construct that reports expression from the *rebP1P2* promoter (P_{rebP1}) as red (mScarlet) fluorescence and inserted it into a neutral site on the chromosome in WT PA14. We also generated similar strains with mScarlet driven by a constitutive promoter ($P_{PA1/04/03}$-*mScarlet*) or a promoterless sequence in the WT background to use as controls. We grew the WT P_{rebP1} and control reporter strains in shaken liquid batch cultures to examine expression over the growth curve. We found that P_{rebP1} showed modest activity compared to that of the constitutive promoter and that it was expressed specifically in the stationary phase of growth (**Figure 3a**). We then created a dual reporter strain containing P_{rebP1}-*mScarlet* and $P_{PA1/04/03}$-*gfp* and grew it to stationary phase in liquid culture before examination via fluorescence microscopy. This imaging revealed that the low relative fluorescence of the P_{rebP1}-*mScarlet* strain (**Figure 3a**) was not due to low uniform expression but instead to stochastic expression of *rebP1P2*, with mScarlet fluorescence visible in just 0.26% ± 0.006% of the cell population (**Figure 3b**).

Based on the conservation of *rcgA* and *fecI* in *Pseudomonas reb* clusters (**Figure 1b; Supplementary Figure 1; Supplementary File 1**), we reasoned that the encoded transcriptional regulators control expression of *rebP1P2*. To test this, we moved the P_{rebP1}-*mScarlet* construct into the PA14 Δ*rcgA* and Δ*fecI2* mutant backgrounds. We observed P_{rebP1}

activity in WT liquid cultures and colony biofilms that was dependent on the presence of *rcgA* and *fecI2* (**Figure 3c, d, Supplementary Figure 4**). Deletion of one or both of these putative regulatory genes resulted in abrogation of *rebP1P2* expression, indicating that RcgA and FecI2
150 are both required for P_{rebP1} activity. Complementation of these genes back into their endogenous loci restored P_{rebP1} expression (**Figure 3c, d and Supplementary Figure 4**).

Because biofilm development leads to the formation of steep chemical gradients that can affect gene expression patterns along the z-axis [19], we chose to visualize P_{rebP1} activity across colony
155 depth. To do this, we employed a thin sectioning protocol to prepare vertical sections taken from the center region of three-day-old colony biofilms [20]. Confocal microscopy of the dual reporter (P_{rebP1}-*mScarlet* $P_{PA1/04/03}$-*gfp*) biofilm sections revealed that cells expressing *rebP1P2* are present in thin striations such that both bright and dark cells are situated at the same depth (**Figure 3d**). The constitutive reporter ($P_{PA1/04/03}$-*gfp*) showed fluorescence that is more
160 consistent between cells at the same depth (**Figure 3c, d**). In agreement with our findings for liquid culture, P_{rebP1}-driven expression in biofilms appears to be stochastic. The vertical arrangement of P_{rebP1}-active cells may indicate that expression status is heritable during vertical growth in the biofilm.

165 In many hosts and various infection sites in humans, biofilm formation by pathogens such as *P. aeruginosa* is critical to bacterial colonization and virulence. Biofilm formation also exacerbates the challenge of treating resistant infections. Matrix secretion is a defining feature of biofilms; the matrix functions as the “glue” that holds bacterial cells together and can facilitate attachment to the host [21,22]. Having observed R-body production by PA14 biofilms, we sought to examine
170 whether this activity contributes to biofilm development, matrix production, or fitness during biofilm growth. We examined biofilm development using a standardized colony morphology assay, in which the dye Congo red is provided in the medium and binds to biofilm matrix. We found that matrix production and biofilm development were unaltered in the Δ*rebP1P2* mutant (**Figure 3e**). Furthermore, Δ*rebP1P2* showed no fitness disadvantage when grown in mixed-
175 strain colony biofilms with the WT parent (**Figure 3f**).

rebP1P2 *is expressed and contributes to PA14 pathogenicity in plant and nematode hosts*

The fact that homologs of the *C. taeniospiralis* R-body structural genes are found in diverse
180 free-living bacteria suggests that their roles extend beyond endosymbiotic interactions [16]. To

examine whether *rebP1P2* is expressed during interactions with hosts, we employed the P_{rebP1}-*mScarlet* reporter strain in *Arabidopsis thaliana* seedling and *Caenorhabditis elegans* gut colonization assays. In both hosts, as in colony biofilms, *rebP1P2* expression patterns were distinct from those exhibited by a promoter driving constitutive expression of mScarlet ($P_{PA1/04/03}$-*mScarlet*). While constitutive mScarlet production was uniform and fuzzy across colonized regions of hosts (**Figure 4a, b**), *rebP1P2* expression was punctate and restricted to a subset of PA14 cells (**Figure 4a**, **b**). The distinct *rebP1P2* expression patterns we observed in the colony biofilm and host contexts may indicate that there is an advantage to restricting R-body production to a subset of cells in the population.

In *C. taeniospiralis* and the plant symbiont *Azorhizobium caulinodans*, R-body production has been linked to host toxicity [4,13,14], and *P. aeruginosa* forms biofilms and acts as an extracellular pathogen during colonization of a range of hosts including plant and nematode models [23,24]. We hypothesized that R-bodies contribute to PA14 host colonization and/or pathogenicity and therefore performed established assays to test such contributions of PA14 R-body production in our two host systems. In *A. thaliana*, we quantified the extent to which PA14 WT and mutant strains colonized seedlings after inoculation and five days of plant growth. For the *C. elegans* virulence assay, we quantified percent survival for up to four days after synchronized populations of worms were exposed to PA14 WT and mutant strains. When compared to WT PA14, Δ*rebP1P2* displayed attenuated host colonization (**Figure 4c**) and virulence (**Figure 4d**); both phenotypes were restored to WT levels upon complementation of *rebP1P2* (**Figure 4c, d**). In combination with the results of our biofilm competition assays (**Figure 3f**), these results indicate that the effects of R-body production are specific to the host-associated lifestyle.

Discussion

We have identified genes required for R-body production by *P. aeruginosa* PA14. In *C. taeniospiralis*, the proteins RebA, RebB, and RebD have been implicated in R-body production. While these proteins are homologous to each other, RebD is an outlier in that it is shorter than RebA and RebB and in that its expression is not required for R-body production. PA14 contains one homolog to RebD, and two RebB homologs that we have designated as “RebP1” and “RebP2” due to their distinct phylogenetic grouping. Similar to the case in *C. taeniospiralis*, RebP1 and RebP2 are longer than PA14 RebD, and RebP1 and RebP2 were both detected in SDS-insoluble preparations from PA14 biofilms, while RebD was not. Expression of the putative

215 *rebP1P2* operon is regulated by the transcription factor RcgA and sigma factor FecI2. RcgA and FecI2 had previously been associated with virulence [12,17], but their exact roles have eluded definition. We have also provided evidence that *rebP1P2* expression is stochastic and that it can be observed both in independent biofilms and during association with hosts. While expression patterns between these two systems appear to be similar, an advantage to R-body production is
220 detectable only during host colonization, suggesting that R-body function is specific to infection.

Though R-body production was initially thought to be limited to parasitic bacteria [25], it has since been shown that *reb* gene homologs are found in diverse proteobacteria, including many non-symbionts [16]. Our results indicate that R-bodies made by *P. aeruginosa* PA14 contribute to
225 colonization of a plant host and to virulence in a *C. elegans* model of infection. In a recent study, the regulator RcgA was found to be necessary for *C. elegans* ribosomal injury that occurs during PA14 infection [26]. Together with our findings, the results of this study hint at a role for R-bodies in releasing a bacterial enzyme, or activating a host enzyme, that cleaves *C. elegans* rRNA. Aside from *C. taeniospiralis*, and now *P. aeruginosa*, to our knowledge a role for R-bodies in
230 host damage has been observed only for the plant symbiont *A. caulinodans.* The *reb* genes in this plant symbiont are repressed by the regulatory protein PraR under both free-living and host-associated conditions, but deletion of PraR allows R-body production and leads to killing of host plant cells [14]. Because R-body production has not been observed in wild type *A. caulinodans*, its significance in the context of bacterium-plant symbiosis is unclear [14]. Nevertheless, the fact that
235 the damaging effects of R-bodies have now been described for three divergent bacterial species hints at a general role for these structures in interactions between proteobacteria and eukaryotes.

Caedibacter R-body extension is triggered by low pH and occurs in phagosomes of naive
240 paramecia, prompting *Caedibacter* lysis and the release of other toxins within *Caedibacter* cells and thereby killing the eukaryotic predator [4,5]. We speculate that PA14 R-body extension is similarly triggered in a host-specific manner and that cells in the R-body-producing subpopulation act as “kamikazes” to release other bacterial products that facilitate colonization and enhance virulence. Our findings raise the possibility that R-body production contributes to
245 the behaviors of diverse free-living bacteria via analagous mechanisms during association with other organisms.

Methods

250

Bacterial strains and growth conditions. Strains used in this study are listed in **Supplementary Table 1**. Cultures of *Pseudomonas aeruginosa* strain UCBPP-PA14 (PA14; [27] were grown in lysogeny broth (LB; 1% tryptone, 1% NaCl, 0.5% yeast extract [28] in 13 mm x 100 mm culture tubes at 37°C with shaking at 250 rpm unless otherwise indicated. Biological replicates were
255 inoculated from distinct clonal-source colonies grown on LB + 1.5% agar plates. Overnight precultures were grown for 14-16 h and subcultures were prepared by diluting precultures 1:100 in LB in 13 mm x 100 mm culture tubes and growing at 37˚C with shaking at 250 rpm until mid-exponential phase (OD at 500 nm ~ 0.5). Subcultures were used in experiments unless otherwise noted.

260

Construction of mutant strains. Markerless deletion and complementation strains were made as described previously [29]. Briefly, ~ 1 kb of flanking sequence from each side of the target locus were amplified using the primers listed in **Supplementary Table 2** and inserted into pMQ30 through gap repair cloning in *Saccharomyces cerevisiae* InvSc1 [30]. Each plasmid, listed in
265 **Supplementary Table 2**, was transformed into *Escherichia coli* strain UQ950, verified by restriction digests and sequencing, and moved into *P. aeruginosa* PA14 using biparental conjugation. PA14 single recombinants were selected on LB agar plates containing 100 µg/ml gentamicin. Double recombinants (markerless mutants) were selected on a modified LB medium (containing 10% sucrose and lacking NaCl) and genotypes were confirmed by PCR.
270 Combinatorial mutants were constructed by using single mutants as hosts for biparental conjugation as indicated in **Supplementary Table 1**.

Phylogenetic analysis. All trees were generated with Geneious Prime 2020.2.4 using Muscle for sequence alignment and the neighbor-joining method for tree building (genetic distance model:
275 Jukes-Cantor (**Supplementary Figure 1**); Tamura-Nei (**Supplementary Figure 2**)). Trees in Figure 1a and **Supplementary Figure 2** were displayed using the online Interactive Tree Of Life (iTOL) tool [31].

Construction of PA14 reporter strains. A transcriptional reporter for the *rebP1P2* operon was
280 constructed using primers listed in **Supplementary Table 2** to amplify the promoter region (500 bp upstream of the *rebP1P2* operon), adding an SpeI digest site to the 5' end and an EcoRI digest site to the 3' end of the promoter. Purified PCR products were digested and ligated into the

multiple cloning site of the pLD3208 vector, upstream of the *mScarlet* coding sequence. This plasmid (pLD3210) was transformed into *E. coli* UQ950, verified by sequencing, and integrated
285 into a neutral site in the PA14 genome using biparental conjugation with *E. coli* S17. PA14 single recombinants were selected on M9 minimal medium agar plates (47.8 mM Na_2HPO_4•$7H_2O$, 22 mM KH_2PO_4, 8.6 mM NaCl, 18.6 mM NH_4Cl, 1 mM $MgSO_4$, 0.1 mM $CaCl_2$, 20 mM sodium citrate, 1.5% agar) containing 100 µg/ml gentamicin. The plasmid backbone was resolved out of PA14 using FLP-FRT recombination by introduction of the pFLP2 plasmid [32] and selected on M9
290 minimal medium agar plates containing 300 µg/ml carbenicillin and confirmed on LB agar plates without NaCl and modified to contain 10% sucrose. The presence of *mScarlet* in the final clones was confirmed by PCR. To create the strain that constitutively expresses *mScarlet*, the constitutively expressing synthetic *lac* promoter ($P_{PA1/03/04}$) was ligated into pLD3208 and mating the resulting plasmid, pLD3433, into the *glmS* locus of the PA14 genome via triparental mating
295 with *E. coli* donor strain BW29427 and *E. coli* helper strain ß2155.

Colony biofilm morphology assays. Ten µl of liquid subcultures were spotted onto 60 mL of colony morphology medium (1% tryptone, 1% agar containing 40 µg/mL Congo red dye and 20 µg/mL Coomassie blue dye) in 100mm x 100mm x 15mm square Petri dishes (LDP D210-16).
300 Plates were incubated for up to five days in the dark at 25°C with >90% humidity (Percival CU-22L) and imaged daily with an Epson Expression 11000XL scanner. Images shown are representative of at least six biological replicates.

Competition mixing assays. OD at 500 nm of subcultures were determined in a Synergy 4 plate
305 reader (BioTek) and subcultures were mixed together in a 1:1 ratio of fluorescent, mScarlet-expressing and non-fluorescent cells. Ten µl of this mixture were spotted onto colony morphology medium and grown as described above. After three days, biofilms were harvested, resuspended in 1 mL of 1% tryptone, and homogenized in an Omni Bead Ruptor 12 bead mill homogenizer for 99 s on the “high” setting. Serial dilutions of homogenized cells were plated onto 1% tryptone +
310 1.5% agar plates and grown overnight at 37˚C and colony forming units (CFU) were determined. Fluorescent CFUs were determined by imaging with a Typhoon FLA7000 fluorescent scanner (GE Healthcare).

Purification of SDS-insoluble biofilm fraction. To isolate the sodium dodecyl sulfate-insoluble
315 (SDS-insoluble) fraction of biofilms, we used a PA14 strain defective in producing the main exopolysaccharide Pel (Δ*pelB-G*). Biological replicates of five-day-old colony biofilms (n = 20,

grown on morphology agar as described above) were harvested from the growth medium with a sterile pipette tip, resuspended in 80 mL of sterile phosphate-buffered saline (PBS), and sonicated for 2 x 10 s on ice with the microtip of a Sonifier 250 (Branson). SDS and β-mercaptoethanol
320 were added to final concentrations of 2% and 5%, respectively, and the sample was nutated on a Nutating Mixer (Fisher Scientific 88 861 043) at room temperature (RT; ~ 25˚C) for 60 min. The sample was then transferred into 1.5-mL microfuge tubes and the insoluble fraction spun down at 16,873 x g for 5 min. The supernatant was discarded and the pellets (i.e., the Congo red-binding, SDS-insoluble fraction) were pooled together.
325

Mass spectrometry of SDS-insoluble proteins. The SDS-insoluble pellet was washed three times with Optima water (Fisher Scientific), solubilized in 100 µL of 98% formic acid at room temperature for 1 h. spin-vacuum dried for 1.5 h, washed with 50% methanol and water, and then dissolved in 2% RapiGest (Waters Corp.) with 6 mM DTT. Samples were then sonicated,
330 boiled, cooled, cysteines reduced and alkylated and proteins digested with trypsin as described previously [33]. Liquid Chromatography mass/ spectrometry (120 min runs) was performed with the Synapt G2 (Waters Corp.) in positive resolution/ion mobility mode with proteins identified with ProteinLynx Global Server (PLGS) as described previously [34]. Proteins were also identified and semi-quantitatively measured with a Q Exactive HF (Orbitrap, Thermo Scientific) with
335 Mascot V. 2.5 as described previously [35]. Identification of the most abundant proteins in these preparations by the Q Exactive HF were confirmed by the qualitative orthogonal method (Synapt G2 ion mobility/PLGS analysis). The reference proteome UP000000653 for *Pseudomonas aeruginosa* strain PA14 from UniProt (Release 2015_10, 11/10/2015) was used for all database searches. All raw MS data files will be publicly available at the MassIVE data repository
340 (https://massive.ucsd.edu).

Scanning-electron microscopy. The SDS-insoluble pellet was resuspended in pre-fixative solution (2% paraformaldehyde, 2.5% glutaraldehyde, 0.0075% L-lysine in PBS) and nutated at RT for 30 min in the dark. The pellet was then washed in sterile PBS and fixed in 2.5%
345 glutaraldehyde in PBS at RT for 30 min in the dark. Fixed pellets were washed twice in PBS and dehydrated through a series of 60-min ethanol washes (25%, 50%, 75%, 95%, 3 x 100% ethanol). Samples were visualized with a Helios NanoLab DualBeam 660 (FEI).

Liquid culture growth assays. Overnight precultures were diluted 1:100 in 200 µl of 1% tryptone
350 in a flat bottom, polystyrene, 96-well plate (Greiner Bio-One 655001) and incubated at 25°C with

continuous shaking on the medium setting in a Biotek Synergy 4 or Biotek Synergy H1 plate reader. The expression of mScarlet was assessed by taking fluorescence readings at excitation and emission wavelengths of 569 nm and 599 nm, respectively, every 30 minutes for up to 24 h. Growth was assessed by taking OD readings at 500 nm simultaneously with
355 the fluorescence readings.

Quantification of cells expressing P_{rebP1}-*mScarlet.* Five µl of overnight PA14 cultures were mounted on a 2% agarose pad on a glass slide, and imaged at 63x on a Zeiss Axio Imager D1 epifluorescence microscope with an AxioCam MRm. Five independent fields of views were
360 captured at random for each biological replicate. Number of cells in each image was determined using the MicrobeJ plugin in Fiji [36,37].

Fluorescence visualization in *P. aeruginosa* colony biofilms. For whole-colony fluorescence imaging, ten µl of liquid subcultures were spotted onto 1% tryptone, 1% agar and colony biofilms
365 were grown in the dark at 25°C with >90% humidity (Percival CU-22L). After three days, bright field images and fluorescence images were visualized with a Zeiss Axio Zoom.V16 fluorescence stereo zoom microscope (excitation, 545 nm; emission, 605 nm for imaging of mScarlet; excitation, 488 nm; emission, 509 nm for imaging of GFP).

370 Thin sections of PA14 colony biofilms were prepared as described previously [20]. Briefly, after three days of growth as described above, biofilms were overlaid with 1% agar and sandwiched biofilms were lifted from the bottom layer and fixed overnight in 4% paraformaldehyde in PBS at 25°C for 24 h in the dark. Fixed biofilms were washed twice in PBS and dehydrated through a series of 60-min ethanol washes (25%, 50%, 70%, 95%, 3 x 100% ethanol) and cleared via three
375 60-min incubations in Histoclear-II (National Diagnostics); these steps were performed using an STP120 Tissue Processor (Thermo Fisher Scientific). Biofilms were then infiltrated with wax via two separate 2-h washes of 100% paraffin wax (Paraplast Xtra) at 55˚C, and allowed to polymerize overnight at 4°C. Trimmed blocks were sectioned in 10-µm-thick sections perpendicular to the plane of the biofilm, floated onto water at 45°C, and collected onto slides.
380 Slides were air-dried overnight, heat-fixed on a hotplate for 1 h at 45°C, and rehydrated in the reverse order of processing. Rehydrated colonies were immediately mounted in TRIS-buffered DAPI:Fluorogel (Electron Microscopy Sciences) and overlaid with a coverslip. Differential interference contrast (DIC) and fluorescent confocal images were captured using an LSM800

confocal microscope (Zeiss). At least three biological replicates of each strain were prepared in
385 this manner.

***A. thaliana* colonization assays.** *Arabidopsis thaliana* ecotype Columbia (Col-0) seeds were sterilized using standard bleach protocols [38]. Washed, surface-sterilized seeds were resuspended in 0.1% agar and subjected to 24 h of cold treatment at 4˚C, then plated and
390 germinated on half-strength MS agar medium containing Gamborg vitamins [39]. Seeds were incubated at 22˚C with a 12-h-light/12-h-dark photoperiod (100-150 μE/m^2/s; Percival CU-22L) for three weeks. *A. thaliana* seedlings were then inoculated with PA14 using a flood inoculation assay [40] and incubated under the same light/dark conditions for five days. For visualization of PA14-infected *A. thaliana*, leaves were excised and *mScarlet* fluorescence was visualized with
395 a Zeiss Axio Zoom.V16 fluorescence stereo zoom microscope. For quantification of PA14 colonization of *A. thaliana*, seedlings were harvested, weighed, and surface-sterilized with 1 mL of 5% H_2O_2 in water for 3 min. These seedlings were washed five times with sterile PBS and homogenized in 1 mL of PBS in a bead mill homogenizer on the “high” setting for 99 sec. Serial dilutions of homogenized tissue were plated onto LB agar plates containing 4 μg/ml tetracycline
400 and grown overnight at 37°C to select for *P. aeruginosa*, and CFU counts were quantified.

***C. elegans* pathogenicity assays.** Ten μl of overnight PA14 cultures were spotted onto NGM agar plates [41] and incubated at 24 h at 37˚C, followed by 48 h at 25˚C. Thirty to 35 larval stage 4 (L4) worms were picked onto the PA14-seeded plates and incubated at 25˚C. For visualization of
405 PA14-infected worms, worms were exposed to PA14 for three days, immobilized in 10 mM levamisole in water, mounted on a 2% agarose pad on a glass slide, and imaged at 20x and 63x on a Zeiss Axio Imager D1 epifluorescence microscope with an AxioCam MRm. For pathogenicity killing assays, which were modified from [23], live/dead worms were counted for up to four days after plating onto PA14-seeded plates. *unc-44*(*e362*) worms, which exhibit body movement
410 deficits, were used instead of wild-type to prevent worms from crawling off the plates.

ACKNOWLEDGEMENTS

This study was supported by NIH/NIAID grant R01AI103369, an NSF CAREER
415 award to L.E.P.D., and NSF GRFP grant DGE - 1644869 to B.W. Mass spectrometer acquisition and operations were funded by New York State Stem Cell Science Board (NYSTEM contracts CO2361 and C029159) with matching funds from Columbia University and the Columbia Stem

Cell Initiative (LMB). We thank Jason Reed (UNC Chapel Hill) for providing *A. thaliana* Col-0 seeds, Hillary Callahan (Barnard College) for technical support in growing seedlings, Martin
420 Chalfie for provision of *C. elegans unc-44(e362)*, and Iva Greenwald for technical support with imaging of *C. elegans*. We also thank Zarina Akbary for technical assistance in creating strain LD3137.

Figure 1

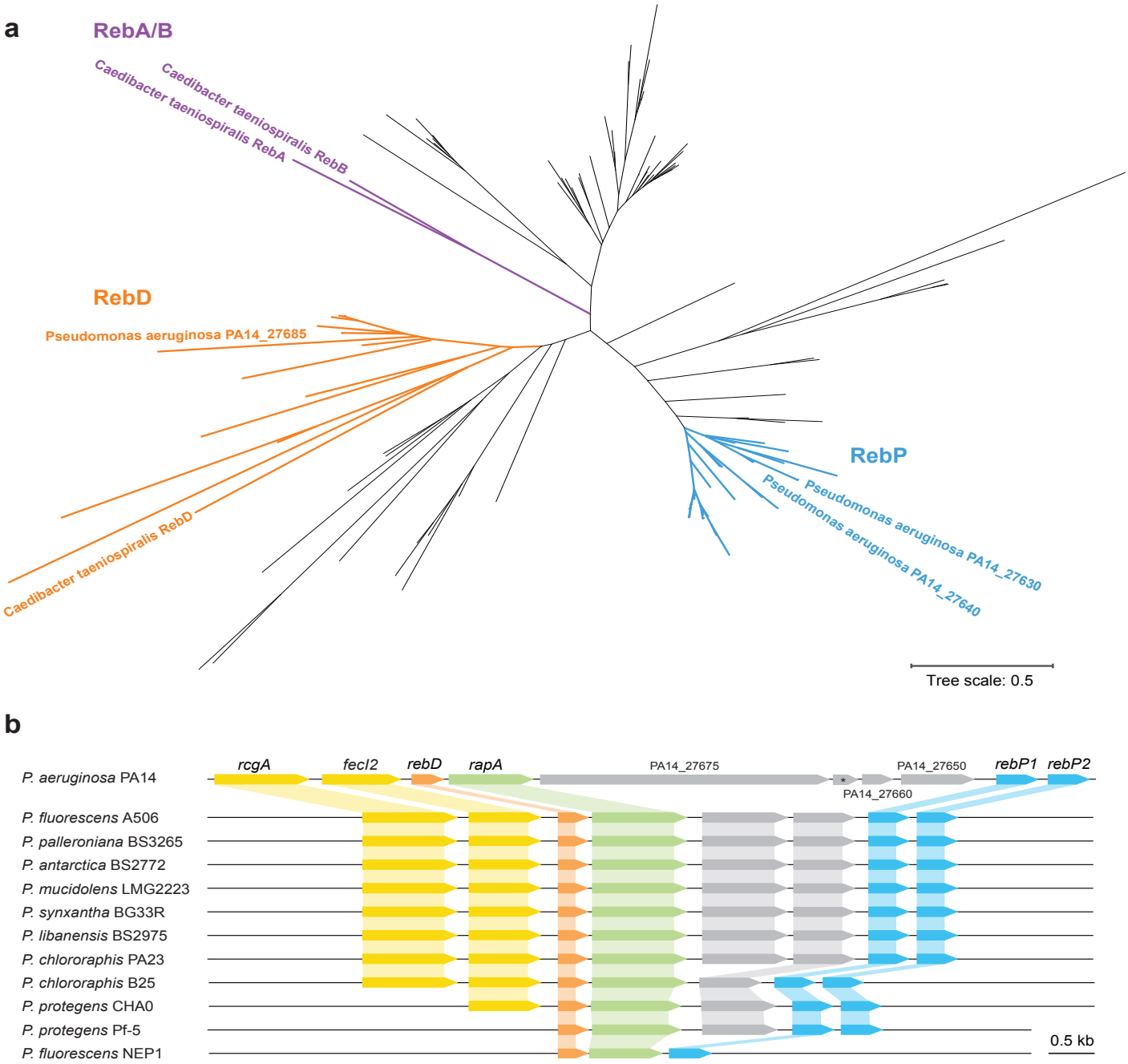

Fig.1. Components of the *reb* gene cluster are found in diverse pseudomonads.
a, Phylogenetic tree of proteins from 38 bacterial strains that are homologous to *C. taeniospiralis* RebB. The bacterial strains included are those with complete genomes from Figure 6 of Raymann *et al*. [16] plus 14 representative pseudomonads (see Figure S1 for the complete annotated tree). *C. taeniospiralis* RebA and RebB are shown in purple. The cluster containing *C. taeniospiralis* RebD and its *Pseudomonas* homologs is shown in orange. We have assigned the designation "RebP" to Reb homologs that cluster with *P. aeruginosa* PA14_27630 and PA14_27640 (shown in blue). **b**, Chromosomal arrangement of genes associated with R-body production in a set of strains that represent all arrangements found in pseudomonads. Regulatory genes are shaded yellow. Genes shaded blue are homologs of *rebP* while genes shaded orange are homologous to *C. taeniospiralis rebD*. *rapA* (*PA14_27680*) and its homologs, which may code for a novel R-body component, are shaded green. The asterisk denotes a gene that is annotated in BioCyc (PA14_RS11205) [42], but not in the Pseudomonas Genome DB [43].

Figure 2

a

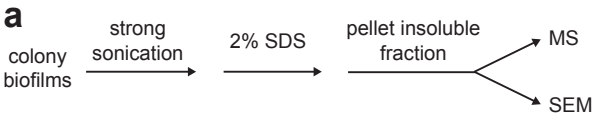

b

Protein Name	Locus (PA14/ PAO1)	Semiquantitative abundance WT	Semiquantitative abundance Δ*pel*
HsiB2	PA14_43040/ PA1657	0.7	11.0
OprF	PA14_41570/ PA1777	6.8	10.4
OprL	PA14_51710/ PA0973	4.3	9.4
-	PA14_06990/ PA0537	1.5	8.4
HsiB3	PA14_34070/ PA2365	0.4	5.0
HsiC2	PA14_43030/ PA1658	0.5	4.9
HsiC3	PA14_34050/ PA2366	1.7	3.8
RplT	PA14_28680/ PA2741	0.0	2.9
-	PA14_50740/ PA1053	1.9	2.6
-	**PA14_27680**	**0.6**	**2.1**
RebP2	**PA14_27630**	**0.8**	**1.4**
RebP1	**PA14_27640**	**0.8**	**1.4**
AlgP	PA14_69370/ PA5253	0.2	1.3
OprM	PA14_05550/ PA0427	0.0	1.2
Pnp	PA14_62710/ PA4740	0.0	1.1
-	PA14_70400/ PA5333	0.3	1.0
PchI	PA14_09320/ PA4222	0.5	0.8
FusA1	PA14_08820/ PA4266	0.0	0.8
-	**PA14_27675**	**0.0**	0.7
LecB	PA14_20610/ PA3361	0.0	0.5

c

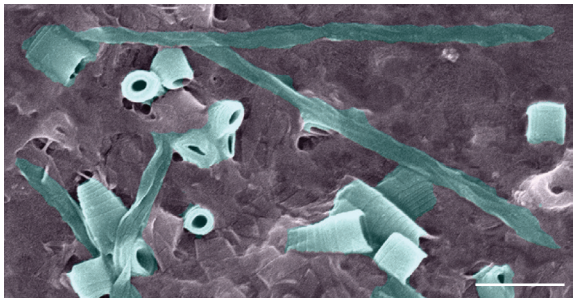

e

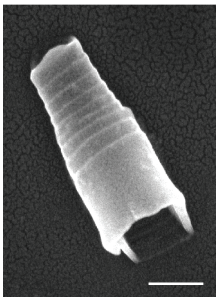

d

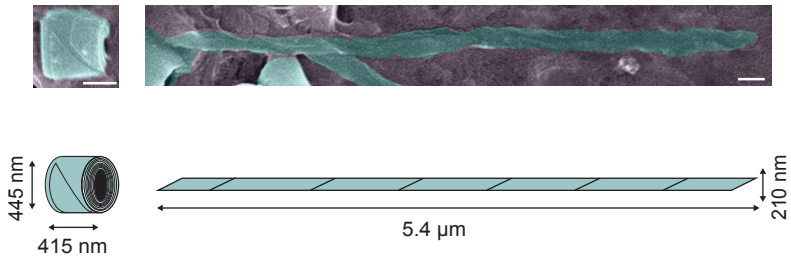

Fig 2. R-bodies are produced by *Pseudomonas aeruginosa* PA14 biofilms. a, Schematic showing method for preparation of SDS-insoluble material from PA14 biofilms. **b**, Top 20 most abundant proteins detected in the SDS-insoluble, formic acid-solubilized fraction of WT (one replicate) and Δ*pel* (two biological replicates) biofilms by mass spectrometry (MS). **c**, Scanning electron micrograph (SEM) image of R-bodies (false-colored turquoise) in the WT sample prepared as shown in **a**. Scale bar is 1 µm. **d**, SEM images, cartoon representations, and dimensions of individual selected R-bodies in fully coiled and fully extended states. Scale bars is 250 nm. **e**, SEM image of a single, partially extended R-body. Scale bar is 400 nm.

Figure 3

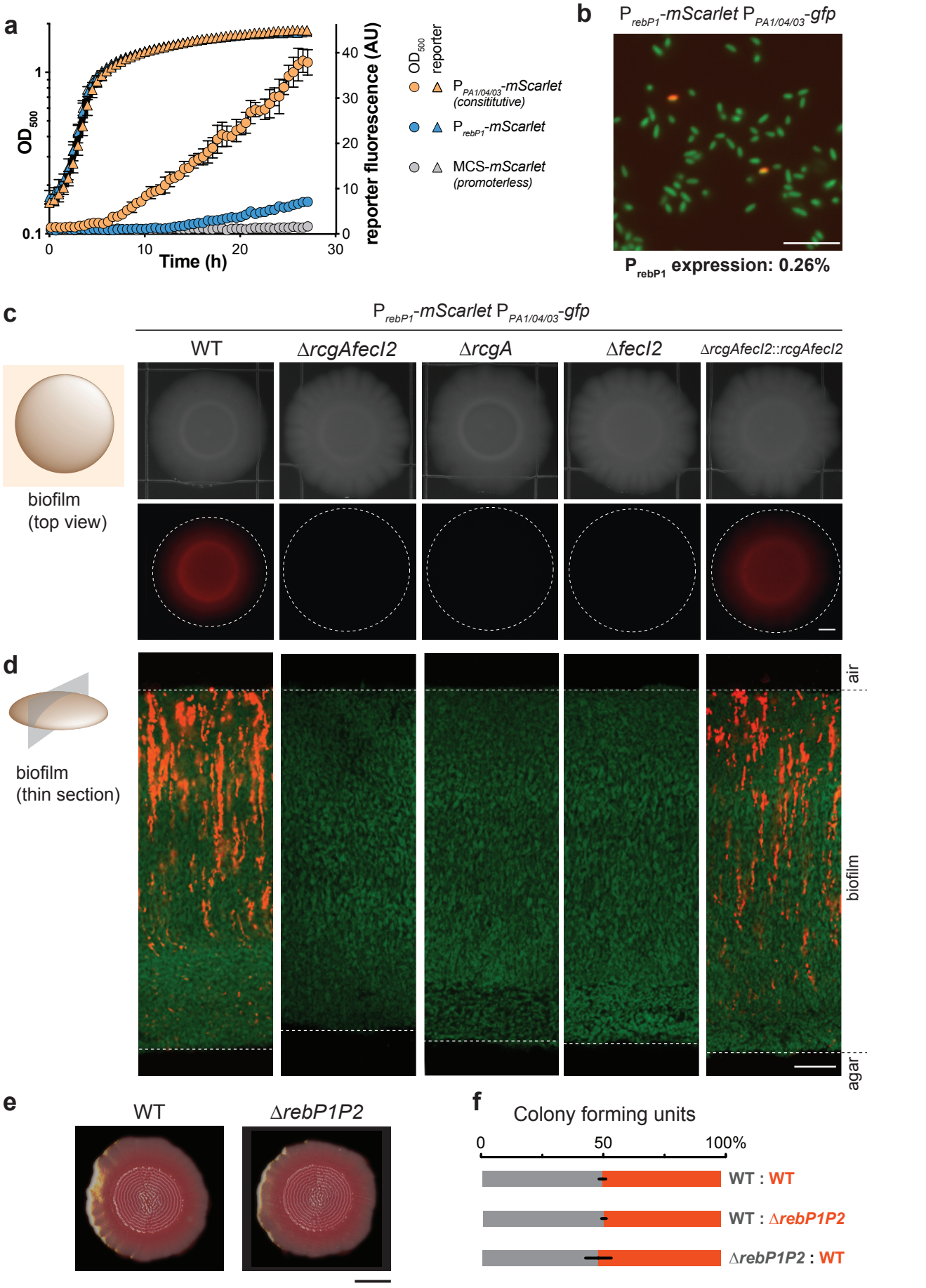
a
OD500
1
0.1
0
10
20
30
Time (h)
reporter fluorescence (AU)
40
30
20
10
0
OD500
reporter
PPA1/04/03-mScarlet (consititutive)
PrebP1-mScarlet
MCS-mScarlet (promoterless)
b
PrebP1-mScarlet PPA1/04/03-gfp
PrebP1 expression: 0.26%
c
PrebP1-mScarlet PPA1/04/03-gfp
WT
ΔrcgAfecI2
ΔrcgA
ΔfecI2
ΔrcgAfecI2::rcgAfecI2
biofilm
(top view)
d
biofilm
(thin section)
air
biofilm
agar
e
WT
ΔrebP1P2
f
Colony forming units
0
50
100%
WT : WT
WT : ΔrebP1P2
ΔrebP1P2 : WT

Fig 3. Expression of PA14 R-body genes is stochastic and controlled by RcgA and FecI2, and does not confer a competitive advantage during growth in biofilms. **a**, Reporter strain growth and expression of mScarlet under the control of the *rebP1P2* promoter (P_{rebP1}-*mScarlet*), no promoter (MCS-*mScarlet*), or a constitutive promoter ($P_{PA1/04/03}$-*mScarlet*) in shaken 1% tryptone liquid cultures incubated at 25 °C. **b**, Fluorescent image of PA14 cells containing P_{rebP1} transcriptional reporter construct (P_{rebP1}-*mScarlet*) and a constitutive promoter driving *gfp* ($P_{PA1/04/03}$-*gfp*) in shaken 1% tryptone liquid cultures grown at 25 °C for 16 h. Image is representative of 6 replicates from three experiments. Scale bar is 20 μm. **c**, Left: Schematic indicating plane of view for right-hand panels. Right: Bright-field and fluorescence microscopy images of three-day-old biofilms formed by the indicated genotypes, containing the P_{rebP1} transcriptional reporter construct (P_{rebP1}-*mScarlet*) and constitutively expressing GFP (via $P_{PA1/04/03}$-*gfp*). Dotted lines demarcate the edges of biofilms. Scale bar is 2 mm. **d**, Left: Schematic indicating plane of view for right-hand panels. Right: Representative images of thin sections prepared from three-day-old biofilms formed by the strains as indicated for **c**. Dotted lines denote the interfaces with air (top) and agar (bottom). Scale bar is 20 μm. **e**, Three-day-old WT and Δ*rebP1P2* biofilms grown on colony morphology medium. Images are representative of nine replicates from three experiments. Scale bar is 4 mm. **f**, Relative percentages of colony forming units (CFUs) of each strain obtained from mixed-strain colony biofilms grown for three days. Each mixed biofilm contained one unlabeled strain and one constitutively expressing mScarlet. Error bars represent standard deviation of biological triplicates.

Figure 4

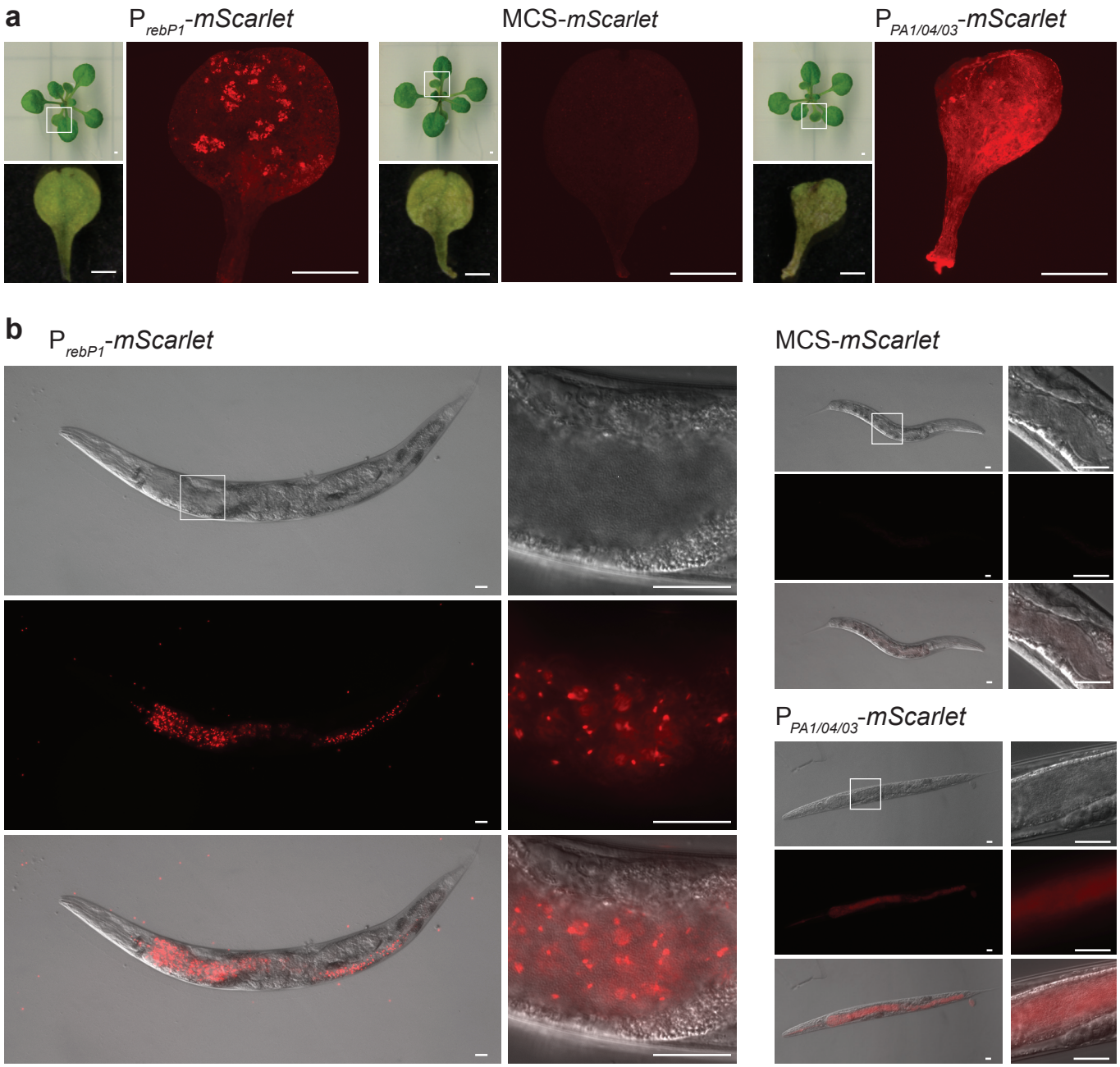
a
P rebP1-mScarlet
MCS-mScarlet
P PA1/04/03-mScarlet
b
P rebP1-mScarlet
MCS-mScarlet
P PA1/04/03-mScarlet
c
Recovered P. aeruginosa (log CFU/mg)
p=0.72
p=0.0007
WT
ΔrebP1P2
ΔrebP1P2::rebP1P2
d
Live Worms (%)
Time (h)
WT
gacA::Tn
ΔrebP1P2
ΔrebP1P2::rebP1P2
<0.0001
<0.0001
<0.0047

Fig. 4. *rebP1P2* is expressed during host association and contributes to host colonization and killing. **a**, Fluorescent micrographs of *A. thaliana* leaves infected with WT PA14 expressing mScarlet under the control of the *rebP1P2* promoter (P_{rebP1}-*mScarlet*), no promoter (MCS-*mScarlet*), or a constitutive promoter ($P_{PA1/04/03}$-*mScarlet*). Smaller panels show images of the whole seedling and the imaged leaf indicated by the white box. Images are representative of nine biological replicates from three experiments. Scale bars are 1 mm. **b**, Images of *C. elegans* fed WT PA14 containing the indicated reporter constructs. Top panels, Nomarski; middle panels, fluorescence; bottom panels, overlay. White boxes indicate regions shown in close-up images. Images are representative of 15 replicates from three experiments. Scale bars are 10 µm. **c**, CFUs obtained from *A. thaliana* seedlings inoculated with the indicated genotypes and incubated for five days, normalized to seedling weight. Each circle represents a biological replicate, with color intensity indicating replicates from the same experiment; colored lines indicate means. p-values were calculated using unpaired, two- tailed t-tests. **d**, Killing kinetics of *C. elegans* following exposure to various PA14 genotypes. The role of *gacA* in *C. elegans* pathogenicity has been described previously [27] and *gacA::Tn* therefore serves as a control for defective killing in this assay. Error bars denote standard deviation and p-values were calculated using unpaired, two-tailed t-tests. $n \geq 4$ biological replicates from three experiments.

REFERENCES

1. Quackenbush, R. L. & Burbach, J. A. Cloning and expression of DNA sequences associated with the killer trait of Paramecium tetraurelia stock 47. *Proc. Natl. Acad. Sci. U. S. A.* **80**, 250–254 (1983).
2. Gibson, I. A comparison of the refractile bodies (R-bodies) of certain bacteria—III. Nucleotide sequence homologies and R-body function. *Micron and Microscopica Acta* **15**, 253–259 (1984).
3. Gibson, I., Bedingfield, G., Dobbs, H. & Shackleton, J. Effects of various agents on the R bodies of certain bacteria. *Micron and Microscopica Acta* **18**, 71–75 (1987).
4. Pond, F. R., Gibson, I., Lalucat, J. & Quackenbush, R. L. R-body-producing bacteria. *Microbiol. Rev.* **53**, 25–67 (1989).
5. Jurand, A., Preer, J. R. & Rudman, B. M. Further investigations on the prelethal effects of the killing action of kappa containing killer stocks of Paramecium aurelia. *J. Exp. Zool.* **206**, 25–47 (1978).
6. Sonneborn, T. M. Mating Types in Paramecium Aurelia: Diverse Conditions for Mating in Different Stocks; Occurrence, Number and Interrelations of the Types. *Proc. Am. Philos. Soc.* **79**, 411–434 (1938).
7. Heruth, D. P., Pond, F. R., Dilts, t. J. A. & Quackenbush, R. L. Characterization of Genetic Determinants for R Body Synthesis and Assembly in Caedibacter taeniospiralis 47 and 116. *J. Bacteriol.* **176**, 3559–3567 (1994).
8. Kanabrocki, J. A., Quackenbush, R. L. & Pond, F. R. Organization and expression of genetic determinants for synthesis and assembly of type 51 R bodies. *J. Bacteriol.* **168**, 40–48 (1986).
9. Pirritano, M. *et al.* Dual-Seq reveals genome and transcriptome of Caedibacter taeniospiralis, obligate endosymbiont of Paramecium. *Sci. Rep.* **10**, 9727 (2020).
10. Schulz, S. *et al.* Elucidation of sigma factor-associated networks in Pseudomonas aeruginosa reveals a modular architecture with limited and function-specific crosstalk. *PLoS Pathog.* **11**, e1004744 (2015).
11. Lee, D. G. *et al.* Genomic analysis reveals that Pseudomonas aeruginosa virulence is combinatorial. *Genome Biol.* **7**, R90 (2006).

12. Vasquez-Rifo, A., Veksler-Lublinsky, I., Cheng, Z., Ausubel, F. M. & Ambros, V. The Pseudomonas aeruginosa accessory genome elements influence virulence towards Caenorhabditis elegans. *Genome Biol.* **20**, 270 (2019).
13. Preer, J. R., Jr, Preer, L. B. & Jurand, A. Kappa and other endosymbionts in Paramecium aurelia. *Bacteriol. Rev.* **38**, 113–163 (1974).
14. Matsuoka, J.-I. *et al.* A putative TetR-type transcription factor AZC_3265 from the legume symbiont Azorhizobium caulinodans represses the production of R-bodies that are toxic to eukaryotic cells. *Soil Sci. Plant Nutr.* **63**, 452–459 (2017).
15. Mikkelsen, H., McMullan, R. & Filloux, A. The Pseudomonas aeruginosa reference strain PA14 displays increased virulence due to a mutation in ladS. *PLoS One* **6**, e29113 (2011).
16. Raymann, K., Bobay, L.-M., Doak, T. G., Lynch, M. & Gribaldo, S. A genomic survey of Reb homologs suggests widespread occurrence of R-bodies in proteobacteria. *G3* **3**, 505–516 (2013).
17. Feinbaum, R. L. *et al.* Genome-wide identification of Pseudomonas aeruginosa virulence-related genes using a Caenorhabditis elegans infection model. *PLoS Pathog.* **8**, e1002813 (2012).
18. Polka, J. K. & Silver, P. A. A Tunable Protein Piston That Breaks Membranes to Release Encapsulated Cargo. *ACS Synth. Biol.* **5**, 303–311 (2016).
19. Stewart, P. S. & Franklin, M. J. Physiological heterogeneity in biofilms. *Nat. Rev. Microbiol.* **6**, 199–210 (2008).
20. Cornell, W. C. *et al.* Paraffin Embedding and Thin Sectioning of Microbial Colony Biofilms for Microscopic Analysis. *J. Vis. Exp.* (2018) doi:10.3791/57196.
21. Donlan, R. M. Biofilms: microbial life on surfaces. *Emerg. Infect. Dis.* **8**, 881–890 (2002).
22. Flemming, H.-C. *et al.* Biofilms: an emergent form of bacterial life. *Nat. Rev. Microbiol.* **14**, 563–575 (2016).
23. Tan, M. W., Mahajan-Miklos, S. & Ausubel, F. M. Killing of Caenorhabditis elegans by Pseudomonas aeruginosa used to model mammalian bacterial pathogenesis. *Proc. Natl. Acad. Sci. U. S. A.* **96**, 715–720 (1999).
24. Walker, T. S. *et al.* Pseudomonas aeruginosa-plant root interactions. Pathogenicity, biofilm formation, and root exudation. *Plant Physiol.* **134**, 320–331 (2004).
25. Heckmann, K. & Görtz, H.-D. Prokaryotic Symbionts of Ciliates. in *The Prokaryotes: A Handbook on the Biology of Bacteria: Ecophysiology, Isolation, Identification, Applications* (eds. Balows, A., Trüper, H. G., Dworkin, M., Harder, W. & Schleifer, K.-H.) 3865–3890 (Springer New York, 1992).

26. Vasquez-Rifo, A., Ricci, E. P. & Ambros, V. Pseudomonas aeruginosa cleaves the decoding center of Caenorhabditis elegans ribosomes. *PLoS Biol.* **18**, e3000969 (2020).
27. Rahme, L. G. *et al.* Use of model plant hosts to identify Pseudomonas aeruginosa virulence factors. *Proc. Natl. Acad. Sci. U. S. A.* **94**, 13245–13250 (1997).
28. Bertani, G. Lysogeny at mid-twentieth century: P1, P2, and other experimental systems. *J. Bacteriol.* **186**, 595–600 (2004).
29. Okegbe, C. *et al.* Electron-shuttling antibiotics structure bacterial communities by modulating cellular levels of c-di-GMP. *Proc. Natl. Acad. Sci. U. S. A.* **114**, E5236–E5245 (2017).
30. Shanks, R. M. Q., Caiazza, N. C., Hinsa, S. M., Toutain, C. M. & O'Toole, G. A. Saccharomyces cerevisiae-based molecular tool kit for manipulation of genes from gram-negative bacteria. *Appl. Environ. Microbiol.* **72**, 5027–5036 (2006).
31. Letunic, I. & Bork, P. Interactive Tree Of Life (iTOL) v4: recent updates and new developments. *Nucleic Acids Res.* **47**, W256–W259 (2019).
32. Hoang, T. T., Karkhoff-Schweizer, R. R., Kutchma, A. J. & Schweizer, H. P. A broad-host-range Flp-FRT recombination system for site-specific excision of chromosomally-located DNA sequences: application for isolation of unmarked Pseudomonas aeruginosa mutants. *Gene* **212**, 77–86 (1998).
33. Oswald, E. S., Brown, L. M., Bulinski, J. C. & Hung, C. T. Label-free protein profiling of adipose-derived human stem cells under hyperosmotic treatment. *J. Proteome Res.* **10**, 3050–3059 (2011).
34. Yang, W. S. *et al.* Regulation of ferroptotic cancer cell death by GPX4. *Cell* **156**, 317–331 (2014).
35. Wobma, H. M. *et al.* The influence of hypoxia and IFN-γ on the proteome and metabolome of therapeutic mesenchymal stem cells. *Biomaterials* **167**, 226–234 (2018).
36. Ducret, A., Quardokus, E. M. & Brun, Y. V. MicrobeJ, a tool for high throughput bacterial cell detection and quantitative analysis. *Nat Microbiol* **1**, 16077 (2016).
37. Schindelin, J. *et al.* Fiji: an open-source platform for biological-image analysis. *Nat. Methods* **9**, 676–682 (2012).
38. Clough, S. J. & Bent, A. F. Floral dip: a simplified method forAgrobacterium-mediated transformation ofArabidopsis thaliana. *The Plant Journal* vol. 16 735–743 (1998).
39. Murashige, T. & Skoog, F. A Revised Medium for Rapid Growth and Bio Assays with Tobacco Tissue Cultures. *Physiologia Plantarum* vol. 15 473–497 (1962).
40. Ishiga, Y., Ishiga, T., Uppalapati, S. R. & Mysore, K. S. Arabidopsis seedling flood-

inoculation technique: a rapid and reliable assay for studying plant-bacterial interactions. *Plant Methods* **7**, 32 (2011).

41. Brenner, S. The genetics of Caenorhabditis elegans. *Genetics* **77**, 71–94 (1974).
42. Karp, P. D. *et al.* The BioCyc collection of microbial genomes and metabolic pathways. *Brief. Bioinform.* **20**, 1085–1093 (2019).
43. Winsor, G. L. *et al.* Enhanced annotations and features for comparing thousands of *Pseudomonas* genomes in the Pseudomonas genome database. *Nucleic Acids Res.* **44**, D646–53 (2016).